Ising field theory in a magnetic field: φ^3 coupling at $T > T_c$

Hao-Lan Xu and Alexander Zamolodchikov

C.N. Yang Institute for Theoretical Physics, State University of New York at Stony Brook, Stony Brook, NY 11794-3840, U.S.A.

E-mail: hao-lan.xu@stonybrook.edu, alexander.zamolodchikov@stonybrook.edu

ABSTRACT: We study the "three particle coupling" $\Gamma^1_{11}(\xi)$, in $2d$ Ising Field Theory in a magnetic field, as the function of the scaling parameter $\xi := h/(-m)^{15/8}$, where $m \sim T_c - T$ and $h \sim H$ are scaled deviation from the critical temperature and scaled external field, respectively. The "φ^3 coupling" Γ^1_{11} is defined in terms of the residue of the $2 \to 2$ elastic scattering amplitude at its pole associated with the lightest particle itself. We limit attention to the High-Temperature domain, so that m is negative. We suggest "standard analyticity": $(\Gamma^1_{11})^2$, as the function of $u := \xi^2$, is analytic in the whole complex u-plane except for the branch cut from $-\infty$ to $-u_0 \approx -0.03585$, the latter branching point $-u_0$ being associated with the Yang-Lee edge singularity. Under this assumption, the values of Γ^1_{11} at any complex u are expressed through the discontinuity across the branch cut. We suggest approximation for this discontinuity which accounts for singular expansion of Γ^1_{11} near the Yang-Lee branching point, as well as its known asymptotic at $u \to +\infty$. The resulting dispersion relation agrees well with known exact data, and with numerics obtained via Truncated Free Fermion Space Approach. This work is part of extended project of studying the S-matrix of the Ising Field Theory in a magnetic field.

Contents

1 Introduction

In this work we report the next step in the extended project of studying the analytic properties of the thermodynamic and correlation characteristics of the 2d Ising Field Theory (IFT) in a magnetic field, as the functions of complex scaling parameter. We understand the IFT as the Ising conformal field theory (CFT) perturbed by its two relevant operators, the energy density $\varepsilon(x)$ and the spin density $\sigma(x)$, as defined by the formal action

$$\mathcal{A}_{\text{IFT}} = \mathcal{A}_{\text{CFT}} + \frac{m}{2\pi} \int \varepsilon(x) d^2 x + h \int \sigma(x) d^2 x \,. \tag{1.1}$$

In [1] the analyticity of free energy was analysed in both High- and Low-Temperature regimes. Analyticity of the correlation length $R_c := M_1^{-1}$ (M_1 stands for the mass of the lightest particle of the theory) was addressed in more recent work [2], albeit only in the High-T regime (the Low-T regime turns out to be more difficult; we plan to return to this problem in the future). It was argued in [2] that the correlation length, as the function of complex scaling parameter, is analytic on the complex plane of this parameter, the only singularity being the so called Yang-Lee edge singularity, the branching point resulting from condensation of the Yang-Lee zeros in the thermodynamic limit. We refer to this analytic property as the "standard analyticity".

In this work we extend the analysis of [2] to the"φ^3 coupling — the quantity which controls the large-distance behaviour of the three point correlation function. As in [2], we limit attention to the High-T domain. We argue that the φ^3 coupling also enjoys the standard analyticity. Our approach here is very similar to the analysis in [2], and we often borrow notations from that paper.

Clearly, the Yang-Lee edge singularity plays the central role in our study. We refer the reader to the works [3–6] for recent developments in this area.

φ^3 coupling. We denote A_1 the lightest stable particle of the theory, and M_1 its mass. Also, as in [2], we use the notation $S_{11}(\theta)$ the S-matrix element of the $A_1 + A_1 \to A_1 + A_1$ elastic scattering. It is a function of the rapidity difference θ. In IFT $S_{11}(\theta)$ always has a pole at $\theta = 2i\pi/3$ corresponding to the particle A_1 itself in the direct channel. (There is of course the associated cross-channel pole at $\theta = i\pi/3$.) The φ^3 coupling Γ_{11}^1 is usually defined in terms of the residue

$$(\Gamma_{11}^1)^2 = -i \operatorname*{Res}_{\theta = \frac{2i\pi}{3}} S_{11}(\theta) \,; \tag{1.2}$$

by this definition $(\Gamma_{11}^1)^2$ is positive in a unitary theory. The vertex Γ_{11}^1 is dimensionless. It depends on the scaling parameter, the dimensionless ratio of the coupling constants m and h in (1.1). As in refs. [1, 2], we use here the ratio $\xi = h/|m|^{15/8}$ (in the High-T domain m is negative). We also use the related parameter $\eta = m/|h|^{8/15} = -\xi^{-8/15}$ when convenient. Because in the High-T regime IFT is unsensitive to the change of the sign of ξ (the change $h \to -h$ in (1.1) can be compensated by the field transformation $\sigma \to -\sigma$), $(\Gamma_{11}^1)^2$ in (1.2) is an even function of ξ,[1] and it is convenient to regard it as function of the variable $u := \xi^2 = h^2/(-m)^{15/8}$. In what follows we use abbreviated notation $\Gamma := \Gamma_{11}^1$, and study the closely related function

$$\kappa(u) := -\frac{\sqrt{3}}{2}\Gamma^2(\xi) = i\frac{\sqrt{3}}{2} \operatorname*{Res}_{\theta = \frac{2i\pi}{3}} S(\theta) \,. \tag{1.3}$$

Here and below $S(\theta)$ is the short-hand for $S_{11}(\theta)$.

The function $\kappa(u)$ can be analytically continued to complex values of u, and understanding the analytic properties of this continuation is the primary goal of the present work. As in [2], our analysis here will be based on the combination of exact results at the integrable points, as well as on the numerical data obtained via Truncated Free Fermion Space Approach (TFFSA) [1].

It is natural to expect that analytic properties of $\kappa(u)$ in the complex u-plane are similar to those of the vacuum energy density $G_{\text{high}}(u)$ [1], and of the mass $M_1(u)$ of the lightest particle A_1 [2]. Namely, one can argue that $\kappa(u)$ is analytic in the whole u-plane with the branch cut from $-\infty$ to $-u_0 = -\xi_0^2 \approx -0.03585\ldots$, as shown in figure 1. We refer to it as the "standard analyticity". The branching point $u = -u_0$ represents the Yang-Lee edge singularity resulting from accumulation of Yang-Lee zeros in the thermodynamic limit [7, 8]. The argument is as follows. Generally, the positions and the residues of the poles of $S(\theta)$ may have, besides the singularity at $-u_0$, additional algebraic singularities (square root branching points) signifying collisions of different poles at special values of u, with two branches of the square root representing interchange of the colliding poles. However, the particular pole at $\theta = 2\pi i/3$ which we are interested in here stays put at all

---

[1]To the contrary, the vertex Γ_{11}^1 itself is an odd function, $\Gamma_{11}^1(-\xi) = -\Gamma_{11}^1(\xi)$. The sign of Γ_{11}^1 is fixed by the condition that Γ_{11}^1 is positive at positive ξ.
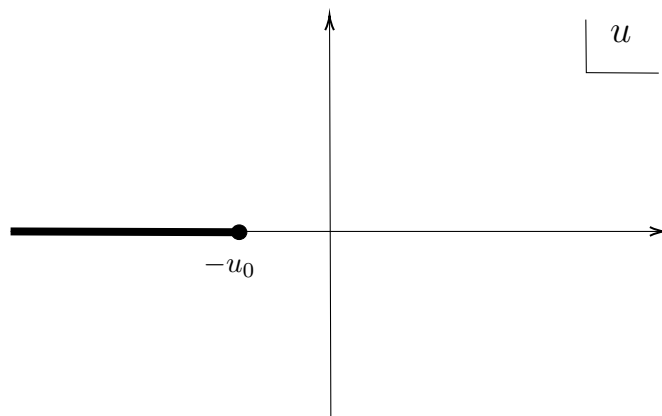
Figure 1. Conjectured "standard analyticity" of $\kappa(u)$ in the complex u-plane: $\kappa(u)$ is analytic everywhere except for the branch cut $[-\infty : -u_0]$. The branching point $-u_0$ is the YL edge singularity. The branch cut represents the shown as the solid line represents the line of first order phase transitions. In particular, the φ^3 coupling is discontinuous across this line.

values of u. There is an interesting movements of other poles and associated zeros under changes of u, as explained in ref. [9]. The choreography of those movements is such that the residue (1.2) never does evolve singularities. Every time another pole hits the pole at $2\pi i/3$, there is a zero hitting it simultaneously, so that the residue remains regular.

Below we verify this analyticity conjecture using a combination of exact and numerical data. We build an approximation for the discontinuity across the above branch cut. Then the analyticity assumption leads to the dispersion relation, and one can check it against special points where $\kappa(u)$ is known exactly, as well as the numerical estimates obtained using TFFSA. We find reasonable agreement (see section 4 and section 5). Alternative numerical data for $\kappa(u)$ at real positive u was previously obtained in [10] by rather different approach. Our results from the dispersion relation are in good agreement with that numerics as well. All these results support the standard analyticity conjecture formulated above.

2 Special points

The theory (1.1) is exactly integrable at two special points. At $u = 0$ it reduces to a theory of free fermi particles with $S(\theta) = -1$, so that the residue (1.2) vanishes. Away from this point $\kappa(u)$ admits expansion in powers of u,

$$\kappa(u) = \sum_{n=1}^{\infty} \kappa^{(n)} u^n \,, \tag{2.1}$$

with finite radius of convergence. The leading term in this expansion was obtained in [11] via form factor perturbation theory,

$$\kappa^{(1)} = -18\sqrt{3}\,\bar{s}^2 = -57.48165545\ldots \,, \tag{2.2}$$

where $\bar{s} = 2^{1/12}e^{-1/8}\,A_{\mathrm{G}}^{3/2} = 1.35783834\ldots$, and A_{G} is Glaisher's constant [12].

Another important point is $u = \infty$ (i.e. $m = 0$), where the (1.1) becomes an integrable theory with eight stable particles and rich factorizable S-matrices [13].[2] The value of $\kappa(u)$ at $u = \infty$ can be straightforwardly extracted from the S-matrix $S_{11}(\theta)$ (eq. (A.2) in appendix A),

$$\kappa(\infty) = -3\,\frac{\tan(7\pi/15)\tan(11\pi/30)}{\tan(2\pi/15)\tan(3\pi/10)} = -104.6154448\ldots. \tag{2.3}$$

In the vicinity of this point $\kappa(u)$ expands in a convergent series in integer powers of $\eta = -u^{-4/15}$,

$$\kappa(u) = \kappa_0 + \kappa_1\,\eta + \kappa_2\,\eta^2 + \kappa_3\,\eta^3 + \ldots \tag{2.4}$$

where $\kappa_0 := \kappa(\infty)$, see eq. (2.3). In principle, the higher coefficients can be obtained via form factor perturbation theory around the integrable point $u = \infty$. In practice, this can be done for κ_1 (see appendix A),

$$\kappa_1 = -202.04\ldots \tag{2.5}$$

while exact calculations of the higher coefficients are rather difficult. We will estimate some coefficients using numerical data in section 4 and section 5.

Interesting point where IFT (1.1) is "infrared integrable" is the Yang-Lee edge singularity which is located at pure imaginary magnetic field h, i.e. at real negative $u = -u_0$. The position u_0 was estimated in [1, 2, 14], $u_0 \approx 0.035846(4)$. This point is critical in usual sense — the analytic continuation of the mass $M_1(u)$ vanishes at $u = -u_0$, i.e. the correlation length diverges [15]. This means that the deep infrared asymptotic of the theory (1.1) at $u = -u_0$ is described by CFT, which was identified in [16] as the non-unitary minimal CFT $\mathcal{M}_{2/5}$ (in what follows we refer to it as YLCFT). Away from the YL point the theory is gapped, with the mass $M_1(u) \sim (u + u_0)^{5/12}$, while its deep IR asymptotic is described by the so called Yang-Lee QFT (henceforth referred to as YLQFT),

$$\mathcal{A}_{\mathrm{YLQFT}} = \mathcal{A}_{\mathrm{YLCFT}} + i\lambda(u)\int \varphi(x)d^2x\,, \tag{2.6}$$

where $\varphi(x)$ is the only nontrivial scalar primary with the conformal dimensions $\left(-\frac{1}{5}, -\frac{1}{5}\right)$ of the YLCFT. The coupling constant $\lambda = \lambda(u)$ turns to zero at the YL point, $\lambda(-u_0) = 0$, in a regular way $\lambda(u) \sim (u + u_0)$. The YLQFT (2.6) itself is known to be integrable, and its factorizable S-matrix is determined by the $2 \to 2$ elastic amplitude [17]

$$S_{11}^{(\mathrm{YLQFT})}(\theta) = \frac{\sinh\theta + i\sin(2\pi/3)}{\sinh\theta - i\sin(2\pi/3)}\,. \tag{2.7}$$

However, the full theory (1.1) is not integrable even in small vicinity of the YL point, not even at the YL point $u = -u_0$ itself. While at u close to $-u_0$ (2.6) describes deep IR

---

[2]The masses of the eight particles A_p, $p = 1, 2, \ldots, 8$ at this integrable point are proportional to the components of Frobenius vector of the Cartan matrix of the Lie algebra E_8, and the structure of the S-matrices reflects in many ways the properties of the E_8 root system [13]. For this reason we refer to this integrable theory as the "E_8 theory".

asymptotic of the theory (1.1), in the full theory the YLQFT is dressed with an infinite tower of irrelevant operators,

$$\mathcal{A}_{\text{IFT}} \ \rightarrow \ \mathcal{A}_{\text{YLQFT}} + \sum_i a^i \int O_i(x) d^2 x \,, \tag{2.8}$$

which become visible at intermediate scales $R \lesssim M_1^{-1}$. Here O_i are scalar operators of YLCFT with $\Delta_i = \bar{\Delta}_i > 1$; contributions of these operators generally break integrability [2] (we will say more about these operators in section 3 below). While M_1 measured in the units of $|m|$ goes to zero when $u \to -u_0$, the couplings $a^i = a^i(u)$ remain finite in this limit. Equivalently, if measured in the units of M_1, these couplings tend to zero when $u \to u_0$. Therefore, the value of κ at $u = -u_0$ can be read out of the S-matrix (2.7),

$$\kappa(-u_0) = i \frac{\sqrt{3}}{2} \operatorname*{Res}_{\theta = \frac{2i\pi}{3}} S_{11}^{\text{YLQFT}}(\theta) = 3. \tag{2.9}$$

The negative value of Γ^2 at this point reflects non-unitary nature of YLQFT.

3 Singular expansion and TTbar deformation

In the vicinity of the YL point $\kappa(u)$ admits singular expansion in fractional powers of $u+u_0$, generated by the irrelevant operators O_i in the effective action (2.8). Schematically, the structure of the expansion is

$$\kappa(u) = \sum_{n=1}^{\infty} \sum_{i_1,\dots,i_n} H_{i_1,i_2,\dots,i_n} \, a^{i_1}(u) \dots a^{i_n}(u) \, [M_1(u)]^{\delta_{i_1} + \dots + \delta_{i_n}} \tag{3.1}$$

where $-\delta_i = 2(1 - \Delta_i) < 0$ are the mass dimensions of the couplings a^i, and $H_{i_1,\dots,i_n}$ are dimensionless coefficients. While the couplings $a^i(u)$ are regular at $u = -u_0$,

$$a^i(u) = a_0^i + a_1^i \, (u + u_0) + a_2^i \, (u + u_0)^2 + \dots \tag{3.2}$$

the mass $M_1(u)$ turns to zero at $u = -u_0$ in a singular manner, $M_1(u) \sim [\lambda(u)]^{5/12} \sim (u + u_0)^{5/12}$, and further admits expansion in fractional powers of $(u+u_0)$ around the YL point, see [2], and eq. (3.16) below. The terms in (3.1) can be interpreted as the contributions from the perturbative expansion in the couplings $a^i(u)$. Of course, the perturbation theory in the irrelevant operators is non-renormalizable, and by itself it does not unambiguously define the coefficients in (3.1) beyond the linear order in the couplings a^i. (Important exception is the "least irrelevant" operator $T\bar{T}$ whose contributions are unambiguous to all orders in the associated coupling α; we discuss its role below.) Nonetheless, (3.1) shows the nature of the singular expansion of $\kappa(u)$ around the YL singularity.

The list of the scalar irrelevant operators entering the expansion (2.8) can be extracted from the known operator content of YLCFT, a.k.a. the minimal CFT $\mathcal{M}_{2/5}$. We arrange them in order of growing dimensions Δ_i, and exclude total derivatives as they do not contribute to the action (2.8). Then the lowest of the irrelevant operators is

$$(T\bar{T}) := L_{-2}\bar{L}_{-2} I \,, \qquad (\Delta, \bar{\Delta}) = (2, 2) \,. \tag{3.3}$$

It is well known to generate the so-called TTbar deformation of the YLQFT, which makes it possible to treat its contributions to all orders (see [18, 19]), as we will discuss shortly. Let us also display the next three operators,

$$\Xi := L_{-4}\bar{L}_{-4}\varphi\,, \qquad (\Delta, \bar{\Delta}) = (3.8, 3.8)\,, \tag{3.4}$$

$$\Xi_6 = L_{-6}\bar{L}_{-6}\varphi\,, \qquad (\Delta, \bar{\Delta}) = (5.8, 5.8)\,, \tag{3.5}$$

$$(T\bar{T})^3 := L_{-2}^3\bar{L}_{-2}^3 I\,, \qquad (\Delta, \bar{\Delta}) = (6, 6)\,. \tag{3.6}$$

Thus, the least irrelevant terms in (2.8) are

$$(2.8) = \mathcal{A}_{\mathrm{YL\ QFT}} + \frac{\alpha(u)}{\pi^2}\int (T\bar{T})(x)d^2x + \frac{\beta(u)}{2\pi}\int \Xi(x)d^2x$$

$$+\frac{\gamma(u)}{2\pi}\int \Xi_6(x)d^2x + \frac{\alpha_5(u)}{\pi^2}\int (T\bar{T})^3(x)d^2x\ +\ \ldots \tag{3.7}$$

where we used individual notations for the couplings. Like all the couplings in (2.8), the couplings α, β, γ in (3.7) are functions of u, regular at the YL point; they admit convergent expansions around the YL point,

$$\begin{aligned}
\alpha(u) &= \alpha_0 + \alpha_1\,(u+u_0) + \alpha_2\,(u+u_0)^2 + \ldots\,, & -\delta_\alpha &= -2\,,\\
\beta(u) &= \beta_0 + \beta_1\,(u+u_0) + \beta_2\,(u+u_0)^2 + \ldots\,, & -\delta_\beta &= -5.6\,, \qquad (3.8)\\
\gamma(u) &= \gamma_0 + \gamma_1\,(u+u_0) + \gamma_2\,(u+u_0)^2 + \ldots\,, & -\delta_\gamma &= -9.6\,,\\
\alpha_5(u) &= \alpha_{5,0} + \alpha_{5,1}\,(u+u_0) + \alpha_{5,2}\,(u+u_0)^2 + \ldots\,, & -\delta_{\alpha_5} &= -10\,,
\end{aligned}$$

and similarly for further couplings not displayed in (3.7). In (3.8) we also show the mass dimensions of the couplings. The leading coefficients for the first two coupling parameters were determined in [2] (see also [1]),

$$\alpha_0\,|m|^2 = -1.32(5)\,, \qquad \frac{\beta_0}{2\pi}\,|m|^{\frac{28}{5}} = +0.72(6)\,. \tag{3.9}$$

In section 5 below we use TFFSA to obtain numerical estimate (not very precise) $\alpha_1|m|^2 = 18.0(3.5)$ of the first sub-leading coefficient in (3.8). Estimates of higher coefficients in (3.8) are not yet available.

With the account of the three lowest irrelevant operators displayed in (3.7) the expansion (3.1) takes the form

$$\begin{aligned}
\kappa(u) = {}& 3 + H_1\,\alpha(u)M_1^2(u) + H_2\,\alpha^2(u)M_1^4(u)\\
& +H_1^\Xi\,\beta(u)M_1^{\frac{28}{5}}(u) + H_3\,\alpha^3(u)M_1^6(u) + H_4\,\alpha^4(u)M_1^8(u) \qquad (3.10)\\
& + \left(H_2^\Xi\,\alpha(u)\beta(u) + H_1^{\Xi_6}\,\gamma(u)\right)M_1^{\frac{48}{5}}(u) + \left(H_5\,\alpha^5(u) + \tilde{H}_1\,\alpha_5(u)\right)M_1^{10}(u) + \ldots
\end{aligned}$$

where the leading term comes from the exact number (2.9). The omitted terms have the powers of $M_1(u)$ 11.6 and higher. Note that apart from the terms linear in the couplings, (3.10) involves higher powers of α, as well as the term $\alpha\beta$. These are associated with the higher order perturbation theory in α. Generally, such terms can not be determined

within the perturbation theory itself, as they depend on short-distance behavior of the full IFT. However, due to special properties of the operator $(T\bar{T})$ many such terms are uniquely defined. As was already mentioned, this operator generates the TTbar deformation, which allows to collect explicitly the higher order terms in α. We will not explain it here, referring the reader to [18–20]. In particular, the TTbar deformation leads to simple "dressing" of the two-particle elastic S-matrix [18, 20],

$$S^{(\alpha)}(\theta) = \exp\left\{-i\alpha M_1^2 \sinh\theta\right\} S^{(0)}(\theta), \tag{3.11}$$

where $S^{(0)}(\theta)$ is the S-matrix of the undeformed theory.[3] If $S^{(0)}(\theta)$ has a pole at $\theta = 2\pi i/3$, so does the deformed $S^{(\alpha)}(\theta)$, with the residue determined by (3.11). Therefore the "TTBar deformed" $\kappa^{(\alpha)}$ relates to $\kappa^{(0)}$ at $\alpha = 0$ as

$$\kappa^{(\alpha)} = \exp\left\{\frac{\sqrt{3}}{2}\,\alpha\,M_1^2\right\}\kappa^{(0)}. \tag{3.12}$$

In our context only five leading terms of the expansion of the exponential in (3.11) and (3.12) are useful. This is because the higher order terms interfere with the contributions of higher level descendants of the identity operator in the effective action (3.7). Thus, the term $\sim \alpha^5$ mixes with the leading contribution from $(T\bar{T})^3$ (α^5 has the same mass dimension as α_5).[4] For the purpose of this work, the expansion

$$\kappa^{(\alpha)} = \left(1 + \frac{\sqrt{3}}{2}\alpha M_1^2 + \frac{3}{8}\alpha^2 M_1^4 + \frac{\sqrt{3}}{16}\alpha^3 M_1^6 + \frac{3}{128}\alpha^4 M_1^8\right)\kappa^{(0)} + O(\alpha^5) \tag{3.13}$$

is more than sufficient. Here $\kappa^{(0)}$ is given by the expansion (3.10) with $\alpha(u)$ set to zero,

$$\kappa^{(0)}(u) = 3 + H_1^{\Xi}\,\beta(u)\,M_1^{\frac{28}{5}}(u) + H_1^{\Xi_6}\,\gamma(u)\,M_1^{\frac{48}{5}}(u) + O(M_1^{10}). \tag{3.14}$$

The second and the third terms in the r.h.s. of (3.14) are linear in β and γ; these terms express the leading order contributions from the operators Ξ and Ξ_6 in (3.7). As usual, unlike the higher orders, these coefficients are determined unambiguously using the perturbation theory. The calculation involves the four particle form factors of the operators Ξ and Ξ_6, and is rather bulky. We will present detailed calculations elsewhere. Here we just quote the result [21],

$$H^{\Xi} = -\frac{164480625}{100352}\frac{5^{\frac{1}{4}}\pi^{\frac{21}{5}}\,\Gamma\left(\frac{3}{5}\right)\Gamma\left(\frac{2}{3}\right)^{\frac{38}{5}}\Gamma\left(\frac{4}{5}\right)\Gamma\left(\frac{8}{3}\right)^2}{2^{\frac{1}{5}}\Gamma\left(\frac{1}{6}\right)^{10}\Gamma\left(\frac{5}{6}\right)^{\frac{12}{5}}\Gamma(\frac{25}{6})^2} = -0.004876389\ldots. \tag{3.15}$$

---

[3]For "TTbar dressing" of the full S-matrix see [20].

[4]From the point of view of straightforward perturbation theory, the TTbar deformation itself generates an infinite tower of higher descendants of I, which mix with the higher terms in (3.7). Alternatively, one can think of the term $\alpha(T\bar{T})$ as the "germ" of the full TTbar deformation; with this convention (3.11) is exact to all orders in α. Likewise, the term $\alpha_5(T\bar{T})^3$, if understood as the germ of generalized TTbar deformation [18], leads to exact dressing by the factor

$$\exp\left\{-i\alpha M_1^2 \sinh(\theta) - i\alpha_5 M_1^{10}\sinh(5\theta) + \ldots\right\}.$$

One can note that this coefficient is exceedingly small numerically, and it does not have any noticeable effect on the analysis in section 4 and section 5 below. We also have reasons to believe that H^{Ξ_6} is yet smaller. Because of this, in what follows we ignore the β- and γ-contributions in (3.14).

Important ingredient in (3.1) is the mass $M_1(u)$ which enjoys the singular expansion around the YL point [2],

$$\frac{M_1(u)}{|m|} = (u + u_0)^{\frac{5}{12}} \left(b(u) + (u + u_0)^{\frac{5}{6}} c(u) + (u + u_0)^{\frac{5}{3}} e(u) + (u + u_0)^{\frac{7}{3}} d(u) + \dots \right), \tag{3.16}$$

where $b(u), c(u), d(u), e(u) \dots$ are regular at $u = -u_0$,

$$b(u) = b_0 + b_1 (u + u_0) + b_2 (u + u_2)^2 + \dots \tag{3.17}$$

$$c(u) = c_0 + c_1 (u + u_0) + \dots \tag{3.18}$$

and similarly for $e(u)$, $d(u)$ and the higher coefficient functions. Some lower coefficients in (3.17), (3.18) were determined in [2],

$$b_0 = 4.228(5), \qquad b_1 = 21.9(9), \qquad c_0 = -14.4(6). \tag{3.19}$$

For the Ising effective action near the YL point, eq. (3.7), the expansion (3.1) combined with (3.8), generates expansion of $\kappa(u)$ in fractional powers of $u + u_0$

$$\kappa(u) = 3 + k_1(u + u_0)^{\frac{5}{6}} + k_2(u + u_0)^{\frac{5}{3}}$$
$$+ k_3(u + u_0)^{\frac{11}{6}} + k_4(u + u_0)^{\frac{5}{2}} + k_5(u + u_0)^{\frac{8}{3}} + \dots, \tag{3.20}$$

where the coefficients are expressed in terms of the coefficients of the expansion of $\alpha(u)$ in (3.8), as well as the coefficients in (3.16), e.g.

$$k_1 = \frac{3\sqrt{3}}{2} b_0^2 \alpha_0 \approx -61.3, \tag{3.21}$$

$$k_2 = \frac{9}{8} b_0^2 \alpha_0^2 \approx 35.0, \tag{3.22}$$

$$k_3 = \frac{3\sqrt{3}}{2} (2b_0 b_1 \alpha_0 + \alpha_1) \approx -681, \tag{3.23}$$

where the estimate of α_0, eq. (3.9), is used to produce numerics for k_1 and k_2. Higher k_n involve higher coefficients in (3.9) and (3.16). We give numerical estimate of more k_n in section 4 and section 5.

4 Analyticity and dispersion relation

According to our analyticity conjecture, the function $\kappa(u)$ admits analytic continuation to the complex u-plane, with no singularities except for the branch cut along the real axis from $-\infty$ to $-u_0$, as shown in figure 1. Under this assumption the values of $\kappa(u)$

everywhere in the u-plane are expressed in terms of the discontinuity across the branch cut, $\mathrm{Disc}\,\kappa(u) := \kappa(u+i0) - \kappa(u-i0) = 2i\,\Im m\,\kappa(u+i0)$

$$\kappa(u) = -u \int_{u_0}^{\infty} \frac{dx}{\pi} \frac{\Im m\,\kappa(-x)}{x(x+u)} \tag{4.1}$$

where we have taken into account that $\kappa(0) = 0$. The integral in (4.1) converges because $\Im m\,\kappa(-x) \simeq x^{15/16}$ as $x \to +\infty$, see (2.4). Here we are going to build certain approximation for the discontinuity $\mathrm{Disc}\,\kappa(u)$ and then check the numerics for $\kappa(u)$ obtained via (4.1) against exact numbers in section 2 and section 3. In addition, in the next section we use TFFSA to obtain numerical values of $\kappa(u)$ at generic real $u > -u_0$, and test the dispersion relation against that numerics as well.

We found it convenient to use the scaling variable

$$\eta = -u^{-4/15} \tag{4.2}$$

instead of u, and define

$$\hat{\kappa}(\eta) = \kappa\left((-\eta)^{-15/4}\right). \tag{4.3}$$

The variable transformation maps the u-plane in figure 1 to the wedge

$$-4\pi/15 < \arg(-\eta) < 4\pi/15 \tag{4.4}$$

in the η-plane, with the positive real u mapped to the negative part of the real axis of η, and negative real u mapped to the rays $\eta = y\,e^{\pm 4\pi i/15}$ with negative real y. In these variable, the dispersion relation (4.1) takes the form

$$\hat{\kappa}(\eta) = -\frac{15}{4\pi} \int_0^{Y_0} \frac{y^{\frac{11}{4}}\,\Delta(-y)\,dy}{\left(y^{\frac{15}{4}} + (-\eta)^{\frac{15}{4}}\right)} \tag{4.5}$$

where it is assumed that η lays in the wedge (4.4), and

$$Y_0 = u_0^{-4/15} = 2.4293\ldots. \tag{4.6}$$

The function

$$\Delta(y) = \frac{1}{2i}\left[\hat{\kappa}\left(y\,e^{\frac{4\pi i}{15}+i0}\right) - \hat{\kappa}\left(y\,e^{\frac{4\pi i}{15}-i0}\right)\right] = \Im m\,\hat{\kappa}\left(y\,e^{\frac{4\pi i}{15}+i0}\right) \tag{4.7}$$

represents the discontinuity across the branch cut in figure 1. To make (4.5) useful we need to build some approximation for $\Delta(y)$.

Approximating $\Delta(y)$. As was mentioned in section 2, the function $\hat{\kappa}(\eta)$ admits convergent expansion (2.4) in integer powers of η. This generates expansion of the function (4.7),

$$\Delta(y) = \sum_{n=0}^{\infty} \kappa_n \sin\left(\frac{4\pi n}{15}\right) y^n = \kappa_1 \sin\left(\frac{4\pi}{15}\right) y + \kappa_2 \sin\left(\frac{8\pi}{15}\right) y^2 + \ldots \tag{4.8}$$

The first two coefficients are

$$\Delta(0) = 0, \qquad \Delta'(0) = \kappa_1 \sin\left(\frac{4\pi}{15}\right) = -150.14\ldots, \tag{4.9}$$

where we have used (2.5).

$\hat{b}_0$	$\hat{b}_1$	$\hat{b}_2$	$\hat{c}_0$	$\hat{c}_1$	$\hat{d}_0$	$\hat{e}_0$
3.0754	0.8932	-0.8618	-0.9412	0.7835	0.3134	0.2880

Table 1. Numerical values of the expansion coefficients in eq. (4.14).

On the other hand, $\hat{\kappa}(\eta)$ enjoys the singular expansion near the YL point $y + Y_0 = 0$,

$$\hat{\kappa}(y) = 3 + \epsilon^{\frac{5}{6}} K_1(\epsilon) + \epsilon^{\frac{5}{3}} K_2(\epsilon) + \epsilon^{\frac{5}{2}} K_3(\epsilon) + \epsilon^{\frac{19}{6}} K_4(\epsilon) + \epsilon^{\frac{10}{3}} K_5(\epsilon) + \epsilon^{\frac{25}{6}} K_6(\epsilon) + \cdots, \quad (4.10)$$

Here and below we use the notation $\epsilon := -(y + Y_0)$, so that

$$u + u_0 = -(-y)^{-15/4} + Y_0^{-15/4} = \frac{15}{4} Y_0^{-\frac{19}{4}} \epsilon - \frac{285}{32} Y_0^{-\frac{23}{4}} \epsilon^2 + \dots \quad (4.11)$$

The coefficient functions $K_n(\epsilon)$ in (4.10) are regular around the YL point

$$K_n(\epsilon) = K_n^{(0)} + K_n^{(1)} \epsilon + K_n^{(2)} \epsilon^2 + \cdots. \quad (4.12)$$

Like in (3.20), the coefficients $K_n^{(l)}$ are related in a straightforward way to the coefficients of the expansion of the $(T\bar{T})$ coupling

$$\alpha = \alpha_0 + \hat{\alpha}_1 \epsilon + \hat{\alpha}_2 \epsilon^2 + \dots \quad (4.13)$$

and the mass,

$$M_1/|h|^{\frac{8}{15}} = \epsilon^{\frac{5}{12}} (\hat{b}_0 + \hat{b}_1 \epsilon + \hat{b}_2 \epsilon^2) + \epsilon^{\frac{5}{4}} (\hat{c}_0 + \hat{c}_1 \epsilon) + \epsilon^{\frac{25}{12}} \hat{e}_0 + \epsilon^{\frac{11}{4}} \hat{d}_0 + O\left(\epsilon^{\frac{19}{6}}\right), \quad (4.14)$$

which are obtained by re-expanding (3.8) and (3.16) in terms of ϵ. The coefficient α_0 is the same as in (3.9) while

$$\hat{\alpha}_1 |m|^2 = -0.85 \pm 0.1 \quad (4.15)$$

will be determined in section 5. Moreover, analysis in section 5 suggests that $\hat{\alpha}_2$ is small, and within the (low) accuracy of our numerics we will neglect its contributions. The coefficients $\hat{b}_0$, $\hat{b}_1$, and $\hat{c}_0$ in (4.14) are expressed through the numbers (3.19), see corresponding entries in table 1. Moreover, it was found in [2] that the mass M_1 is approximated well at $y + Y_0 \lesssim 1$ by all six terms explicitly displayed in (4.14), with the numerical values of the coefficients in table 1.

It is straightforward to obtain the expansion of the discontinuity $\Delta(y)$ by termwise analytic continuation $\epsilon \to e^{i\pi}\epsilon$ in (4.10),

$$\Delta(y) = (-\epsilon)^{\frac{5}{6}} \tilde{K}_1(\epsilon) + (-\epsilon)^{\frac{5}{3}} \tilde{K}_2(\epsilon) + (-\epsilon)^{\frac{5}{2}} \tilde{K}_3(\epsilon) + \cdots \quad (4.16)$$

where $\epsilon = y + Y_0$ is now negative ($\Delta(y)$ vanishes at $y < -Y_0$), and

$$\tilde{K}_n(\epsilon) = \sin(\nu_n \pi) K_n(\epsilon), \quad (4.17)$$

with ν_n standing for the exponent in $\epsilon^\nu K_n(\epsilon)$ term in (4.10). Numerical values of the coefficients $\tilde{K}_n^{(l)} = (-)^l \sin(\pi \nu_n) K_n^{(l)}$ at nine leading terms of the expansion (4.16) obtained from the known coefficients in (4.14) and (4.13) are collected in table 2.

$\tilde{K}_1^{(0)}$	$\tilde{K}_2^{(0)}$	$\tilde{K}_1^{(1)}$	$\tilde{K}_3^{(0)}$	$\tilde{K}_2^{(1)}$	$\tilde{K}_1^{(2)}$	$\tilde{K}_4^{(0)}$	$\tilde{K}_5^{(0)}$	$\tilde{K}_3^{(1)}$
2.7481	7.274	-1.103	10.78	-1.400	-1.655	-0.5601	10.47	-0.8974

Table 2. Numerical values of the coefficients in the expansion (4.16) with $\tilde{K}_n(\epsilon) = \sum_{l=0}^{\infty} \tilde{K}_n^l \, \epsilon^l$.
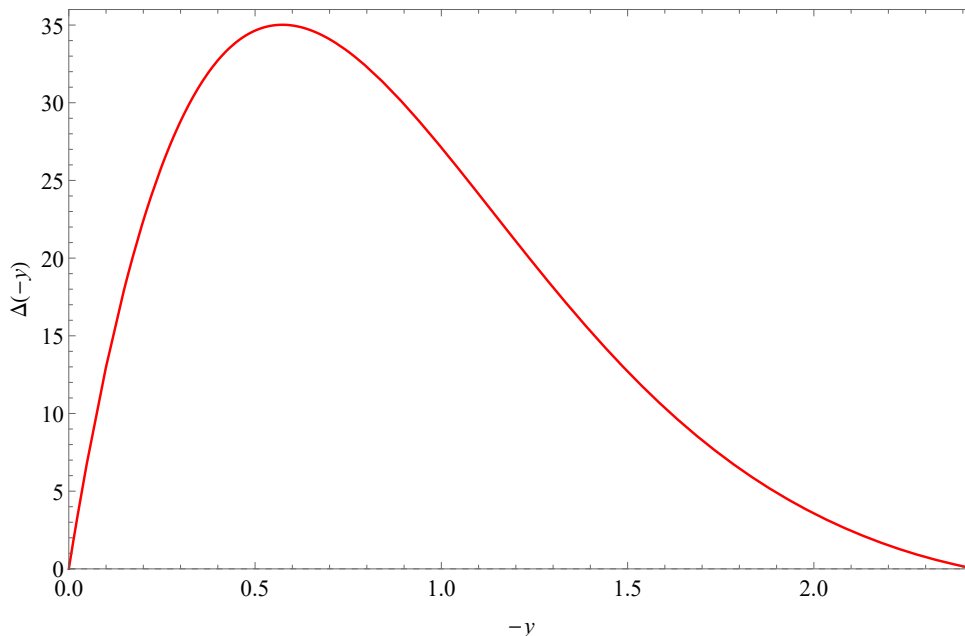

Figure 2. Approximation (4.18) for the discontinuity $\Delta(-y)$ in the dispersion relation (4.5).

We propose the following approximation for $\Delta(y)$ in the whole domain of integration in (4.5):

$$\Delta_{\text{approx}}(y) = \epsilon^{\frac{5}{6}} \tilde{K}_1^{(0)} + \epsilon^{\frac{5}{3}} \tilde{K}_2^{(0)} + \epsilon^{\frac{11}{6}} \tilde{K}_1^{(1)} + \epsilon^{\frac{5}{2}} \tilde{K}_3^{(0)} + \epsilon^{\frac{8}{3}} \tilde{K}_2^{(1)} + \epsilon^{\frac{17}{6}} \tilde{K}_1^{(2)}$$
$$+ \epsilon^{\frac{19}{6}} \tilde{K}_4^{(0)} + \epsilon^{\frac{10}{3}} \tilde{K}_5^{(0)} + \epsilon^{\frac{7}{2}} \tilde{K}_3^{(1)} + \epsilon^{\frac{11}{3}} \tilde{K}_2^{(2)} + \epsilon^{\frac{23}{6}} \tilde{K}_1^{(3)} + \epsilon^{\frac{25}{6}} \tilde{K}_6^{(0)} \,, \qquad (4.18)$$

with $\tilde{K}_1^{(0)}, \ldots, K_3^{(1)}$ taken from table 2, and the last three coefficients $\tilde{K}_2^{(2)}$, $\tilde{K}_1^{(3)}$, and $\tilde{K}_6^{(0)}$ determined by demanding that $\Delta_{\text{approx}}(y)$ meets the two conditions (4.9), and that the dispersion integral (4.5) evaluated with $y = -Y_0$ returns exact value $\hat{\kappa}(-Y_0) = 3$ (see (2.9)),

$$\tilde{K}_2^{(2)} = -182.959 \,, \quad \tilde{K}_1^{(3)} = +238.478 \,, \quad \tilde{K}_6^{(0)} = -66.657 \,. \qquad (4.19)$$

The shape of the function $\Delta_{\text{approx}}(y)$ at $y \in [-Y_0, 0]$ is shown in figure 2. Despite somewhat artificial way of constructing this approximation, we believe that it is very close to actual discontinuity (4.7). This expectation can be verified against exact numbers (section 2) and numerical data obtained in section 5.

Approximation $\Delta_{\text{approx.}}(y)$ vs. data. In constructing the approximation (4.18) we have used the exact slope κ_1, eq. (2.5). However, the leading term $\kappa_0 = \kappa(\infty)$ in (2.4)
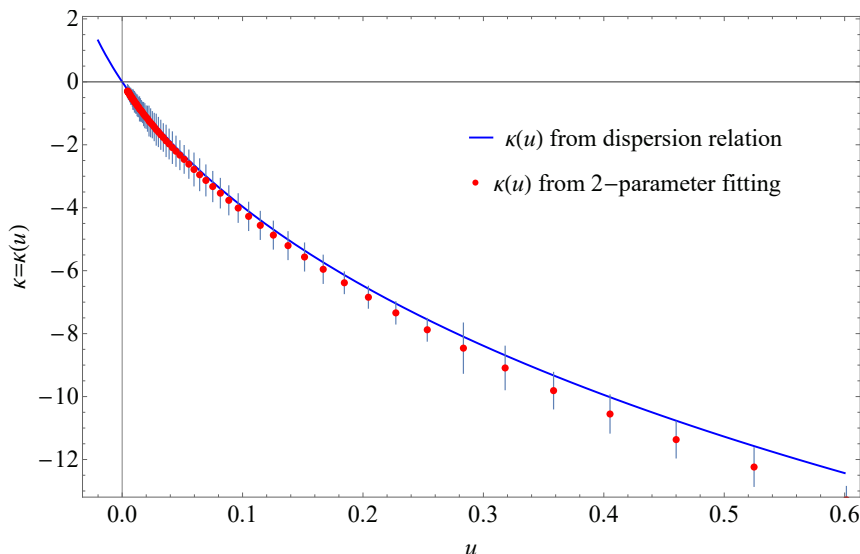
Figure 3. Numerical estimates of $\kappa(u)$ obtained by fitting (5.3) to TFFSA data (red bullets), compared to $\kappa_{\mathrm{disp}}(u)$ from the dispersion relation (4.5) with the approximation (4.18).

does not contribute to the discontinuity. The dispersion integral (4.5) with our approximation (4.18), evaluated at $\eta = 0$, results in

$$\kappa_{\mathrm{disp}}(\infty) = -\frac{15}{4\pi} \int_0^{Y_0} \frac{\Delta_{\mathrm{approx}}(-y)}{y} \, dy = -103.206 \,, \tag{4.20}$$

to be compared with the exact value (2.3). The approximation (4.18) suggests estimates for further coefficients in the expansion (2.1), e.g.

$$\kappa_{2\,\mathrm{disp}} = -213.278 \,, \qquad \kappa_{3\,\mathrm{disp}} = -192.962 \,. \tag{4.21}$$

Another exactly known quantity is the slope (2.2) of $\kappa(u)$ at $u = 0$. The dispersion relation yields

$$\kappa_{\mathrm{disp}}^{(1)} = -\frac{15}{4\pi} \int_0^\infty y^{\frac{11}{4}} \, \Delta_{\mathrm{approx}}(-y) \, dy = -56.9019 \,. \tag{4.22}$$

Again, it agrees well with the exact value (2.2). Our approximation gives predictions for several higher terms of the expansion (2.1),

$$\kappa_{\mathrm{disp}}^{(n)} = (-)^n \, \frac{15}{4\pi} \int_0^\infty y^{\frac{15}{4}\,n-1} \, \Delta_{\mathrm{approx}}(-y) \, dy \,. \tag{4.23}$$

Thus

$$\kappa_{\mathrm{disp}}^{(2)} = 317.754 \,, \qquad \kappa_{\mathrm{disp}}^{(3)} = -3524.51 \,. \tag{4.24}$$

In the next section we will use TFFSA to develop numerics for $\kappa(u)$, both at positive and negative u. Although our numerical estimates are not very precise (we present some details of our numerical analysis in section 5 below), figure 3 we compare them with $\kappa_{\mathrm{disp}}(u)$, the integral (4.5) evaluated with $\Delta_{\mathrm{approx.}}(y)$ in the integrand. The numerics for $g_{111}^2(\eta) := -4\sqrt{3}\,\hat{\kappa}(\eta)$ at negative η (positive u) was previously obtained in [10] using much different analysis of the TFFSA data. We compare these results with $\hat{\kappa}_{\mathrm{disp}}(\eta)$ in figure 4. The agreement seems to support the standard analyticity conjecture.
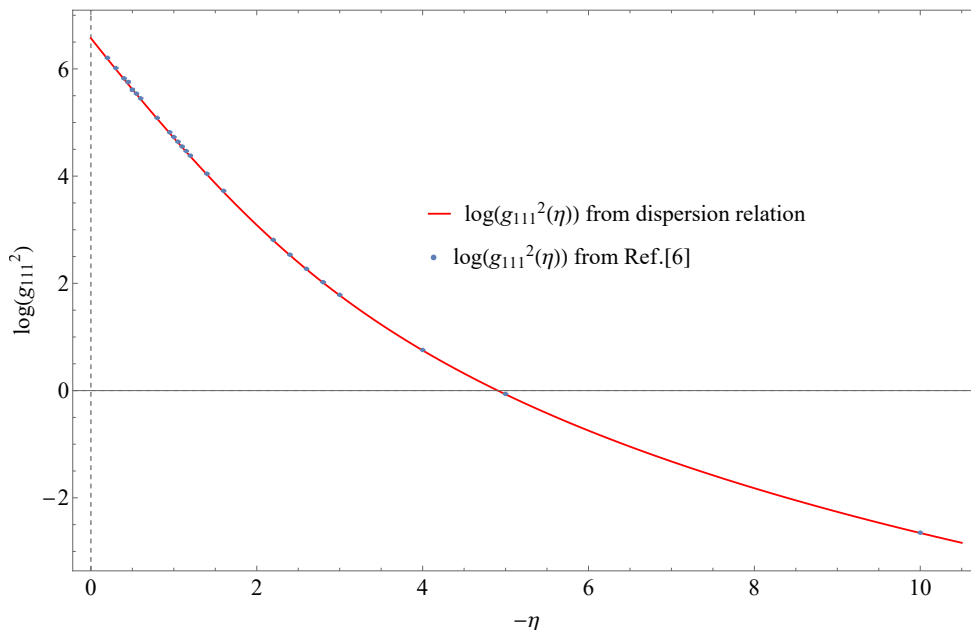
Figure 4. Numerical data for $g_{111}^2(\eta) := -4\sqrt{3}\,\hat{\kappa}(\eta)$ from [10] (blue dots), compared with the same quantity evaluated from the dispersion relation (4.5) with the approximation (4.18) (red curve). For better visibility, we plot $\log(g_{111}^2)$ against $-\eta$.

5 Numerical data from TFFSA

Additional data on $\kappa(u)$ can be obtained numerically, using the TFFSA. As was mentioned, TFFSA was applied previously to estimate the scattering amplitude and in particular the residue (1.3) in [10]. We use different approach, based on the finite-size correction to the two lowest energy levels. TFFSA is a routine which computes the energy levels $E_n(R)$ of the IFT in the geometry of a cylinder, with the spatial coordinate x compactified on a circle of circumference R. With sufficiently high truncation level L TFFSA returns very accurate estimates for $E_n(R)$ as long as $R \lesssim 7\,|h|^{-8/15}$, but at larger R the accuracy quickly deteriorates due to the truncation effects. All numerics quoted below was obtained at the truncation level $L = 13$.[5]

Since in this geometry the lowest excited state $n = 1$ may be interpreted as a single particle A_1 at rest on the circle, the gap $\Delta E_1(R) := E_1(R) - E_0(R)$ is expected to converge to M_1 as $R \to \infty$. Moreover, when $M_1 \neq 0$ the leading finite-size corrections are expressed exactly in terms of the residue (1.3) and the analytic continuation of the amplitude $S(\theta)$ [22],

$$\frac{\Delta E_1(R) - M_1}{M_1} = \kappa\, e^{-\frac{\sqrt{3}}{2}M_1 R} - \int \frac{d\theta}{2\pi} \cosh\theta \left[S\left(\theta + \frac{\pi i}{2}\right) - 1\right] e^{-M_1 R \cosh\theta} + \cdots, \quad (5.1)$$

where the dots represent further corrections which decay yet faster at large R. The two terms in the r.h.s. of (5.1) express contributions of the particle A_1 winding around the

---

[5]Here we assume the same definition of the "truncation level" as given in [1, 2]; it differs by a factor of $1/2$ from the definition in [10].
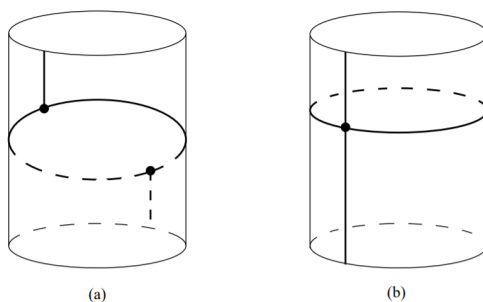
Figure 5. The diagrams are presenting the leading finite size corrections to $\Delta E_1(R)$, see (5.1) and (B.2).
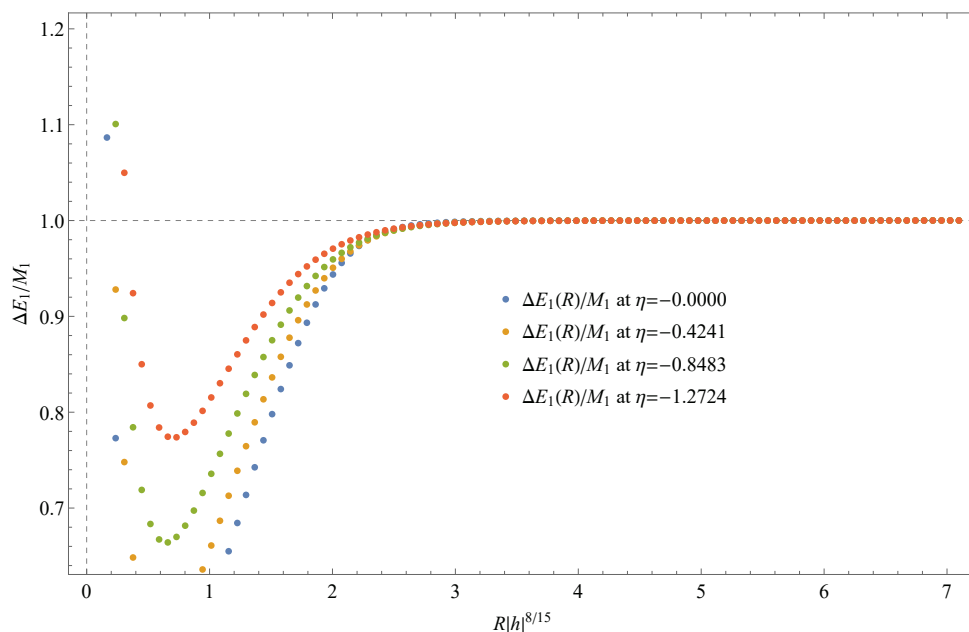

Figure 6. Plots of $\Delta E_1(R)/M_1$ at different η (real h). The exponential approach to 1 is in accord with (5.1) with negative κ.

space-time cylinder once, as shown in figure 5. Other stable particles, when present (as in IFT at $u > u_2 = 0.0640(25)$), lead to additional contributions to the gap (5.1). We describe some of these contributions in appendix B.

The gaps $\Delta E_1(R)$ obtained via TFFSA with $L = 13$, at few sample values of u are shown in figure 6 and figure 7. The exponential approach to M_1 at large R consistent with the leading term in (5.1) is clearly visible, except for when u is close to the YL point $-u_0$ where the behavior at $R \lesssim 7\,|h|^{-8/15}$ becomes rather power-like. Rough estimate of numerical values of $\kappa(u)$ can be obtained by fitting the leading term in the r.h.s. of (5.1) to the TFFSA data.

Unfortunately, precision of such estimate is low. The reason is that truncation effects spoil the TFFSA data for $\Delta E_1(R)$ at large R (typically at $MR \gtrsim 20$) where the leading term in (5.1) dominates. On the other hand, at smaller values of MR the correction terms
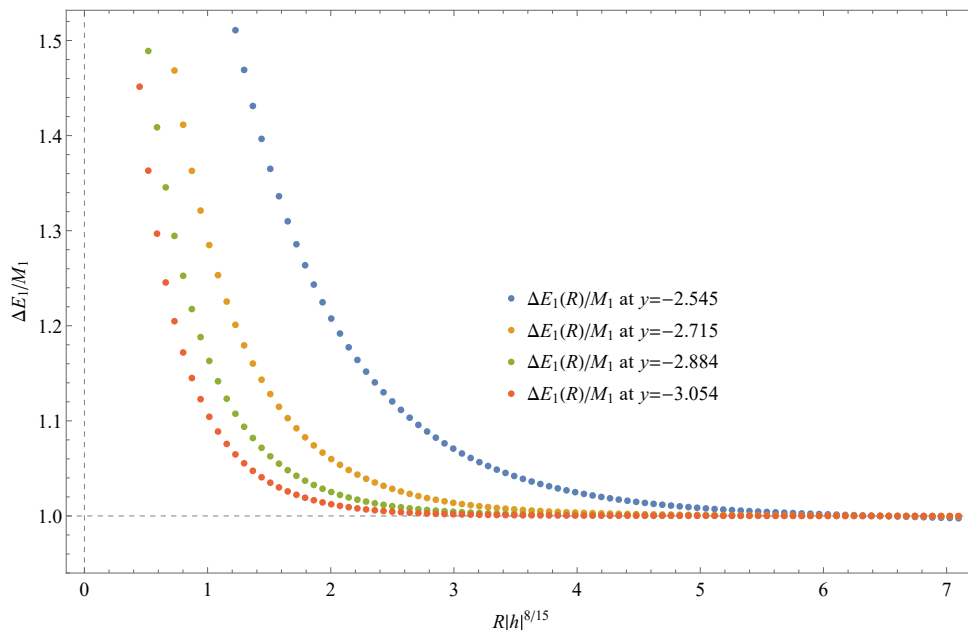
Figure 7. Plots of $\Delta E_1(R)/M_1$ at different y for (imaginary h). The approach to 1 is consistent with (5.1) with positive κ.

in the large R expansion (5.1) become comparable to the leading exponential term. Thus, the second term in the r.h.s. of (5.1) has the leading large-R behavior

$$- \sigma \, (M_1 R)^{-1/2} \, e^{-M_1 R} \,, \tag{5.2}$$

where $\sigma = [S(i\pi/2) - 1]/\sqrt{2\pi}$; with $\sigma \sim \kappa$,[6] the first term dominates only at $MR \gtrsim 10$. Therefore the window in which the above fitting is meaningful is not sufficiently wide, while the fitting results were rather sensitive to the choice of the domain of R where fitting was performed. We estimated the accuracy of this approach by the dependence on the fitting interval to be typically about 15–25%. It can be somewhat improved by fitting the data to the two-parameter expression

$$\kappa \, e^{-\frac{\sqrt{3}}{2} M_1 R} - \sigma \, (M_1 R)^{-1/2} \, e^{-M_1 R} \,, \tag{5.3}$$

via κ and σ. The data presented in figure 3 were obtained through this two-parameter fitting. We estimate the accuracy at generic u as 10–20%.

Accuracy of the estimates obtained using (5.3) deteriorates even more when u is close to one of the three special points mentioned in section 3. Since the correlation length M^{-1} diverges at the YL point, the window available for the fitting shrinks as u approaches $-u_0$. When u is close to zero $\kappa(u) \sim u$ becomes small, and within the acceptable range it is barely detectable on the background of the higher finite-size corrections. In vicinity of the

---

[6]The ratio σ/κ is ≈ -3.2 at $u = +\infty$. It becomes positive at $-0.0036 \lesssim u \lesssim 12.5$ (turning to zero at the boundaries of this segment) and it approaches $-1.7166\ldots$ when $u \to -u_0$. Obviously, this ratio diverges at $u = 0$, where σ remains finite; in some vicinity of this point the ration actually is very large, which makes it difficult to estimate κ near the point $u = 0$.

E_8 point $\eta = 0$ the theory involves more than one stable particle; these additional particles give rise to additional sub-leading terms which are significant in the interval of R available for fitting. However, near these points the accuracy can be significantly improved with the use of exact scattering amplitudes at these points.

Vicinity of free fermion point. At $u = 0$ we are dealing with the free fermion theory, with trivial S-matrix $S(\theta) = -1$ and $\kappa(0) = 0$. In high-T domain, the finite size ground state is the Neveu-Schwarz vacuum, while the first excited state is understood as one particle A_1 at rest over the Ramond vacuum. Therefore, at $u = 0$ the finite size gap is given by

$$\frac{\Delta E_1^{\mathrm{FF}}(R) - M_1}{M_1} = -\int_{-\infty}^{+\infty} \frac{d\theta}{2\pi} \cosh\theta \, \log\left(\frac{1 - e^{-M_1 R \cosh\theta}}{1 + e^{-M_1 R \cosh\theta}}\right), \qquad (5.4)$$

which accounts for contributions from particles A_1 winding around the cylinder any number of times. At small u the amplitude $S(\theta)$ acquires a correction

$$S(\theta) = -\left(1 + \frac{i\kappa A(\theta)}{\sinh\theta}\right), \qquad A(\theta) = A_{\mathrm{pole}}(\theta) + A_\sigma(\theta), \qquad (5.5)$$

where:

$$A_{\mathrm{pole}}(\theta) = -\frac{2}{\sqrt{3}} \frac{\sinh^2\theta}{\sinh^2\theta + \frac{3}{4}}, \qquad (5.6)$$

and the absorptive part $A_\sigma(\theta)$ is determined by the inelastic processes, see [11]. This leads to correction terms to the finite size gap (5.4),

$$\frac{\Delta E_1(R) - M_1}{M_1} = -\int_{-\infty}^{+\infty} \frac{d\theta}{2\pi} \cosh\theta \, \log\left(\frac{1 - e^{-M_1 R \cosh\theta}}{1 + e^{-M_1 R \cosh\theta}}\right)$$
$$+ \kappa\, e^{-\frac{\sqrt{3}}{2} M_1 R} - \frac{2}{\sqrt{3}} \kappa \int \frac{d\theta}{2\pi} A(i\pi/2 + \theta)\, e^{-M_1 R \cosh\theta}. \qquad (5.7)$$

When $M_1 R \gtrsim 1$ the integral in (5.7) is dominated by $\theta \lesssim 1$, where $A_\sigma(\theta)$ is numerically small as compared to $A_{\mathrm{pole}}(\theta)$ (see figure 3 in [11]), and one can neglect its contribution to the finite size gap. Therefore, we have used (5.7) with $A(\theta) = A_{\mathrm{pole}}(\theta)$ to fit TFFSA data via κ. The best fit was obtained in the interval $3.5 < M_1 R < 9.5$, and the result is shown in figure 8, where it is compared to $\kappa_{\mathrm{disp}}(u)$ obtained from the dispersion relation (4.3).

Vicinity of E_8 point. When negative η is sufficiently close to the E_8 point $\eta = 0$, IFT involves more than one stable particle. At $\eta_3 < \eta < 0$, $\eta_3 \approx -0.13$, there are two heavier particles A_2 and A_3, and at $\eta_2 < \eta < \eta_3$, $\eta_2 \approx -2.08$, only one additional stable particle A_2 remains in the spectrum[7] [9]. While the finite-size correction terms displayed in (5.1) describe contributions of the particle A_1 winding once around the cylinder, similar winding of these heavier particles generates further sub-leading terms in the large R expansion

---

[7]There are eight stable particles at $\eta = 0$, see footnote 2 in section 2. When η shifted from zero five of them loose stability and become resonance states.
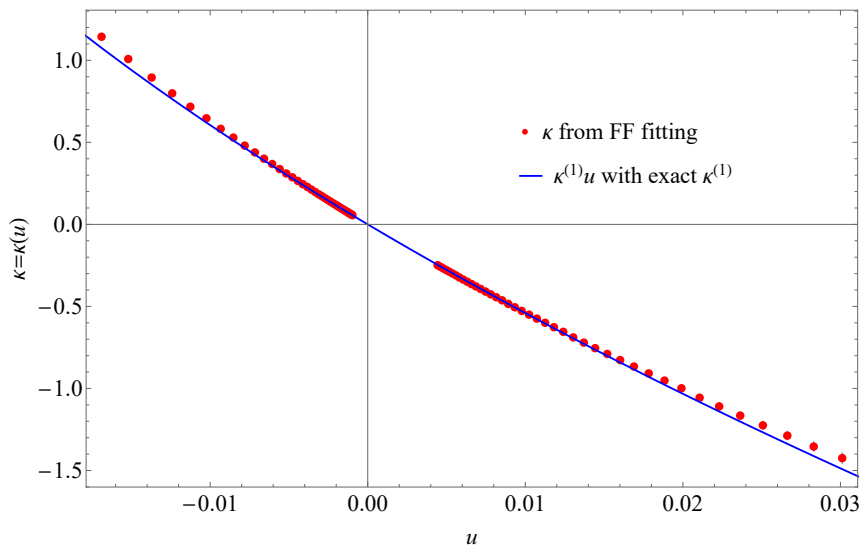
Figure 8. The results of the fitting (5.7) to TFFSA data via κ, at $-0.02 < u < +0.03$, are shown as red bullets. The blue curve is $\kappa_{\text{disp}}(u)$, the integral (4.5) with $\Delta(y)$ given by (4.18).

of $\Delta E_1(R)$,

$$\frac{\Delta E_1(R) - M_1}{M_1} = \kappa\, e^{-\frac{\sqrt{3}}{2}M_1 R} + \kappa_2\, e^{-\mu_{22}^1 R} + \kappa_3\, e^{-\mu_{33}^1 R}$$
$$- \sum_{p=1}^{3} \frac{M_p}{M_1} \int \frac{d\theta}{2\pi} \cosh\theta \left[S_{1p}\left(\theta + \frac{\pi i}{2}\right) - 1 \right] e^{-M_p R \cosh\theta} + O(e^{-2M_1 R}),$$

$$(5.8)$$

where the notations are explained in appendix B. Of course when $\eta < \eta_3$ the terms associated with the particle A_3 (i.e. the exponential term with κ_3 as well as the term with $p = 3$ in the second line in (5.8)) are to be dropped.

We used (5.8) as a fit of the TFFSA data for $\Delta E_1(R)$ at $-0.6 < \eta < 0$. To make (5.8) useful for determining κ one needs to know the masses M_2 and M_3 in this interval. We have determined M_2 and M_3 directly from the TFFSA data for $M_1 R \gg 1$. Also, κ_3 must be set to zero at $\eta < \eta_3$, and moreover one can argue that the parameter κ_3 is rather small at $\eta \in [\eta_3 \ldots 0]$. Indeed, κ_3 must turn to zero at the boundaries of this narrow interval. For that reason we set κ_3 to zero in the whole domain $[-0.6 \ldots 0]$. Finally, we assumed that when η is small the S-matrix elements $S_{1p}(\theta)$ are not too much different from these amplitudes at $\eta = 0$ which are known exactly. With these approximations, κ was determined from the best fit to the TFFSA via two parameters κ and κ_2. In all cases some segments within the window $12.2 < M_1 R < 18.8$ were taken as the fitting domain. This procedure substantially improved the accuracy of the estimate of κ, especially when η is close to zero ($\eta \gtrsim -0.6$). The results are shown in figure 9, where the error bars reflect the dependence on the choice of the fitting interval.

Vicinity of the YL point. When close to the YL point there is a good approximation for the amplitude $S(i\pi/2 + \theta)$ in the second term in (5.1). The main correction due to
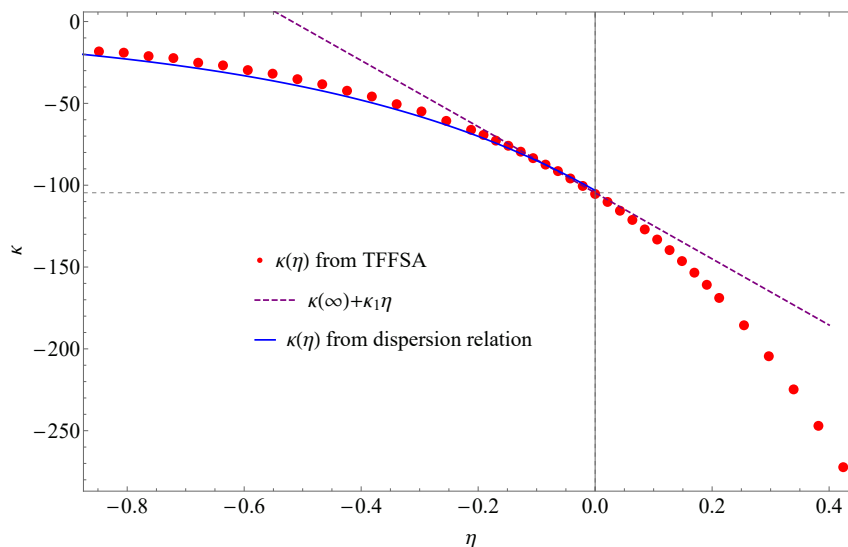
Figure 9. Red bullets show the result of the best fit of $\hat{\kappa}(\eta)$ to TFFSA data for $\Delta E_1(R)$, using (5.8) with κ and κ_2 (κ_3 was set to zero, see main text). The blue curve is $\hat{\kappa}_{\text{disp}}(\eta)$, the integral (4.5) with $\Delta(y)$ given by (4.18), and the magenta dashed line is showing the exact slope κ_1 at E_8 point, see (2.5) and appendix A.

the irrelevant operators in (2.8) to the YLQFT S-matrix (2.7) comes from the operator $(T\bar{T})$ in (3.7). As was explained in section 3, up to the order $\alpha^4 M_1^8 \sim (u + u_0)^{\frac{10}{3}}$, its contribution is identical to the TTbar deformation (3.11), with the $S^{(0)}$ taken to be the YLQFT S-matrix (2.7). Therefore near the YL point (5.1) can be approximated as

$$\frac{\Delta E_1(R) - M_1}{M_1} = \kappa\, e^{-\frac{\sqrt{3}}{2}M_1 R} \tag{5.9}$$
$$- \int \frac{d\theta}{2\pi} \cosh\theta \left[e^{-M_1 R \cosh\theta}\, e^{\alpha M_1^2 \cosh\theta}\, S_{11}^{\text{YLQFT}}\left(\theta + \frac{\pi i}{2}\right) - 1 \right] + \cdots$$

with the mass M_1 given by the expansion (3.16). We also used two term approximation for α,

$$\alpha = \alpha_0 + \hat{\alpha}_1\left(y + Y_0\right), \tag{5.10}$$

with known $\alpha_0 = -1.32$ [2], and adjustable slope α_1. With this approximations of the second term in (5.1) we found that the best fit of (5.1) to the TFFSA data via κ can be obtained with

$$\hat{\alpha}_1 |m|^2 = -0.85 \pm 0.1. \tag{5.11}$$

When the fitting interval was taken within the segment $M_1 R \in [4.0, 7.5]$ the fitting results were stable for $-3.8 < y < -2.8$. As we approached yet closer to the YL point $-Y_0 = -2.4293$ the quality of the fit deteriorated rapidly. The mass $M_1 \simeq 1.602\, \epsilon^{5/6}$ becomes small, and the domain of R where (5.9) is expected to give meaningful approximation is pushed beyond the range where TFFSA data is accurate. The result is shown in figure 10, along with $\tilde{\kappa}(y) := \kappa((-y)^{-15/4})$ from the approximation (3.12) with $\alpha = \alpha_0$ and α given by (5.10).
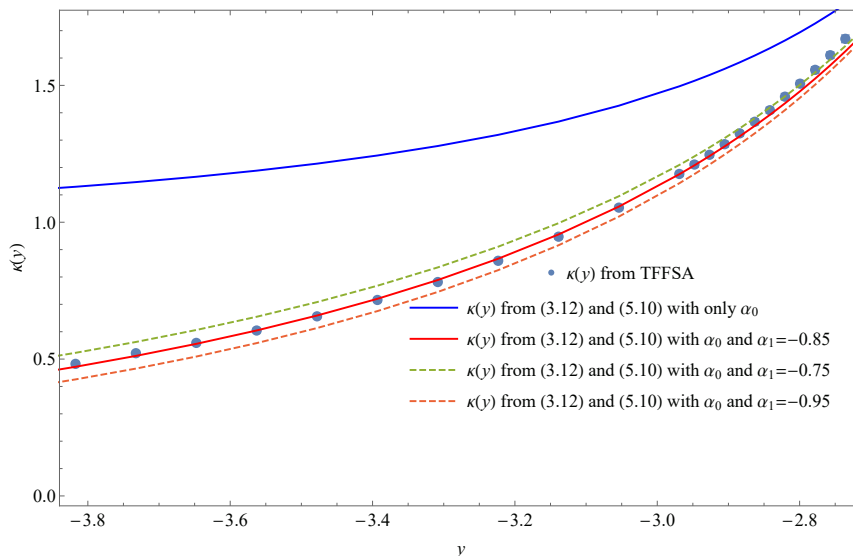
Figure 10. Numerical estimates of $\tilde{\kappa}(y) := \kappa((-y)^{-15/4})$ obtained by fitting (5.9) to TFFSA data via κ (grey bullets). The blue line shows $\tilde{\kappa}(y)$ given by (3.12) with $\kappa^{(0)} = 3$ and set $\alpha \approx \alpha_0 = -1.32 |m|^{-2}$, respectively. The red line is the plot of (3.12) with $\kappa^{(0)} = 3$, and α given by (5.10) with $\hat{\alpha}_1 = -0.85 |m|^{-2}$. The dotted lines show the same function with slightly different values of $\hat{\alpha}_1$.

6 Discussion

In this work we have tested analyticity of the φ^3 coupling $\kappa(u)$ as the function of the scaling parameter $u = h^2/|m|^{\frac{15}{4}}$. Assuming maximal analyticity, we have constructed an approximation for the discontinuity across the branch cut in figure 1, and compared the dispersion relation (4.3) with exact and numerical data available through TFFSA in section 5, and previously in [10]. Agreement supports the analyticity conjecture, as well as the approximation (4.18) for the discontinuity.

As in [2], important tool in our analysis was application of the $T\bar{T}$ deformation formulae, which allowed for control of higher order terms in the coupling parameter $\alpha(u)$ in the effective action (3.7). For $\kappa(u)$ the equation (3.12) reproduces exactly the α-expansion up to terms α^4, leading to the singular expansion (3.13), (3.14). The terms $\sim \alpha^5$ and higher interfere with the contributions from the operators $(T\bar{T})^3 = L^3_{-2}\bar{L}^3_{-2}I$ and higher descendants of identity. We would like to note in this connection that the operator $(T\bar{T})^3$, as well as $(T\bar{T})^4 := L^4_{-2}\bar{L}^4_{-2}I$ and a string of certain higher descendants of identity, generate the "generalized TTbar deformation" [18] (see also [23]) with known effect on the S-matrix. This gives access to yet higher terms in the singular expansion (3.10), and potentially may throw some light on important general question of convergence of the effective action expansion (2.8): does it (or, rather the associated singular expansions like (3.1)) converge in some finite domain around the YL point? We hope to address this intriguing problem in the future.

One of practical outcomes of this work is the first estimate (4.15) of the sub-leading term α_1 in (4.13), which would help to further constrain coefficients in singular expansions

of physical quantities around the YL point. This is important in view of potential application to the problem of "extended analyticity" which would include the low-T domain. Unfortunately, our estimate (4.15) is not too precise, with possible error of about 20%. Further work is required to improve this result, and to determine higher couplings in the effective action (3.7).

We regard this work as a step toward quantitative understanding of how the particle spectrum (including resonance states) and S-matrix of IFT depends on the parameters of the theory. Except of some points in the parameter space, the theory is not integrable, and its S-matrix involve all kinds of inelastic processes. We will address some properties of inelastic amplitudes and resonance states in forthcoming work [21]. Significance of this study is two-fold. First, IFT describes the basic universality class of second order phase transitions (such as the liquid-vapor critical point), and its analysis is important in understanding detailed structure of the associated critical singularity. On the other hand, we develop tools for quantitative description of strongly interacting QFT with rich particle/resonance spectrum and S-matrix.

Acknowledgments

Note added. In forthcoming paper [14] the free energy of IFT in imaginary magnetic field was computed numerically using an improved corner transfer matrix approach. The authors managed to locate the YL singularity at $u_0 = 0.0358536516(1)$, with the precision which seems to be substantially better then our estimate $u_0 = 0.03586(4)$. In addition, they give what appears to be more precise estimate of some of the parameters in the effective action (3.7), particularly the coupling α_0. We are grateful to the authors of [14] for sharing these results prior to publication.

A Derivation of κ_1 in (2.5)

Consider again the $A_1 + A_1 \to A_1 + A_1$ elastic scattering amplitude $S_{11}(\theta)$. This amplitude of course depends on the scaling parameter η, but we suppress this argument to simplify notations. Analytic continuation of this amplitude to complex θ yields the function analytic in the θ-plane with the poles manifesting the bound states, and the branch cuts associated with the inelastic channels $A_1 + A_1 \to X$, where X stands for any states involving more than two of the particles A_1, as well as the higher bound states A_p. The principal branch values of this amplitude enjoy the functional relations

$$S_{11}(\theta)S_{11}(-\theta) = 1, \qquad S_{11}(\theta) = S_{11}(i\pi - \theta), \tag{A.1}$$

which follow from unitarity and analyticity (see e.g. [11] for the details).

At $\eta = 0$ the theory is integrable. We denote $S_{11}^{(0)}(\theta)$ the amplitude at $\eta = 0$. At this integrable point all inelastic channels are closed, and $S_{11}^{(0)}(\theta)$ is a meromorphic function of θ. Its exact form is

$$S_{11}^{(0)}(\theta) := \frac{\sinh\theta + i\sin\frac{2\pi}{3}}{\sinh\theta - i\sin\frac{2\pi}{3}} \frac{\sinh\theta + i\sin\frac{2\pi}{5}}{\sinh\theta - i\sin\frac{2\pi}{5}} \frac{\sinh\theta + i\sin\frac{\pi}{15}}{\sinh\theta - i\sin\frac{\pi}{15}}, \tag{A.2}$$

the poles at $\theta = 2\pi i/3$, $\theta = 2\pi i/5$, and $\theta = i\pi/15$ are the manifestations of the particles A_1, A_2, and A_3 in the direct channel of the scattering, while the poles at $\theta = i\pi/3$, $\theta = 3\pi i/5$, and $\theta = 14\pi i/15$ represent the same particles in the cross channel.[8] Correspondingly, the masses of the particles A_2 and A_3 at $\eta = 0$ are

$$M_2^{(0)} = 2M_1^{(0)}\cos\left(\frac{\pi}{5}\right), \qquad M_2^{(0)} = 2M_1^{(0)}\cos\left(\frac{\pi}{30}\right), \tag{A.3}$$

where $M_1^{(0)}$ is the mass of A_1 at $\eta = 0$.[9]

At nonzero but sufficiently small η the elastic amplitude $S_{11}(\theta)$ admits convergent expansion in powers of η, which we choose to write as

$$S_{11}(\theta) = S_{11}^{(0)}(\theta)\left(1 + \eta\,\Phi^{(1)}(\theta) + \frac{1}{2}\eta^2\,\Phi^{(2)}(\theta) + \dots\right). \tag{A.4}$$

Here we concentrate attention on the first correction term $\eta\varphi^{(1)}(\theta)$, which satisfy the relations

$$\Phi^{(1)}(\theta) = -\Phi^{(1)}(-\theta), \qquad \Phi^{(1)}(\theta) = \Phi^{(1)}(i\pi - \theta), \tag{A.5}$$

in virtue of (A.1). In fact, $\Phi^{(1)}(\theta)$ can be found in a closed form, as follows.

At nonzero η the integrability of IFT is broken, and $S_{11}(\theta)$ develops branching points at the inelastic thresholds. However, the discontinuities of this amplitude across the associated branch cuts are $O(\eta^2)$, and hence $\varphi^{(1)}(\theta)$ in (A.4) remains a meromorphic function of θ. Indeed, the discontinuities across the branch cuts are related in a simple way to the inelastic cross sections, which in turn are proportional to the squares of the absolute values of the inelastic amplitudes. Since at small η the inelastic amplitudes are $O(\eta)$, the discontinuities are $O(\eta^2)$. It is then possible to argue that, up to terms η^2 and higher, the amplitude (A.4) can be written as

$$S_{11}(\theta) = \frac{\sinh\theta + i\sin\frac{2\pi}{3}}{\sinh\theta - i\sin\frac{2\pi}{3}} \frac{\sinh\theta + i\sin\alpha_2}{\sinh\theta - i\sin\alpha_2} \frac{\sinh\theta + i\sin\alpha_3}{\sinh\theta - i\sin\alpha_3} + O(\eta^2), \tag{A.6}$$

where

$$\alpha_2 = \frac{2\pi}{5} + \alpha_2'\,\eta, \qquad \alpha_3 = \frac{\pi}{15} + \alpha_3'\,\eta, \tag{A.7}$$

and α_p', $p = 2, 3$ are numbers, to be determined shortly. In other words, the leading $\sim \eta$ correction to $S_{11}(\theta)$ is determined entirely by the shifts of the positions of the poles (and

---

[8]Although the theory at this integrable point involves eight stable particles, only three lightest particles A_1, A_2, and A_3 appear as the poles in $S_{11}^{(0)}(\theta)$. The remaining particles show up in as the poles in the elastic amplitudes of $S_{pp'}^{(0)}(\theta)$ with p or p' greater than one, see [13] for details.

[9]Closed form expression for the coefficient $M_1^{(0)}/|h|^{\frac{8}{15}}$ can be found in e.g. [2], appendix B.

related zeros) of $S_{11}(\theta)$ associated with the particles A_2 and A_3. Expanding (A.6) to the first order in η one finds

$$\Phi^{(1)}(\theta) = \frac{2i\,\alpha_2'\cos\frac{2\pi}{5}\,\sinh\theta}{\sinh^2\theta + \sin^2\frac{2\pi}{5}} + \frac{2i\,\alpha_3'\cos\frac{\pi}{15}\,\sinh\theta}{\sinh^2\theta + \sin^2\frac{\pi}{15}}\,. \tag{A.8}$$

and hence

$$\kappa_1 = \sqrt{3}\left[\frac{\alpha_2'\cos\frac{2\pi}{5}}{\sin^2\frac{2\pi}{3} - \sin^2\frac{2\pi}{5}} + \frac{\alpha_3'\cos\frac{\pi}{15}}{\sin^2\frac{2\pi}{3} - \sin^2\frac{\pi}{15}}\right]\kappa(\infty)\,, \tag{A.9}$$

where $\kappa_0 = \kappa(\infty)$, see eq. (2.3).

The slopes α_p' in (A.10) are related in a simple way

$$\alpha_p' = \frac{2}{\sqrt{\left(2M_1^{(0)}/M_p^{(0)}\right)^2 - 1}}\left(\frac{M_1^{(1)}}{M_1^{(0)}} - \frac{M_p^{(1)}}{M_p^{(0)}}\right)\,, \tag{A.10}$$

to the leading coefficients in the expansions of the masses M_p of the particles A_p,

$$M_p = M_p^{(0)} + M_p^{(1)}\,\eta + O(\eta^2)\,. \tag{A.11}$$

While $M_p^{(0)}$ are known exactly from the integrable theory, the leading corrections $M_p^{(1)}$ were obtained via the form factor perturbation theory in [24], leading to

$$\alpha_2' = 0.378325\ldots\,, \qquad \alpha_3' = 1.35226\ldots\,. \tag{A.12}$$

With this, (A.9) leads to (2.5).

One could rise two objections to the proposed expression (A.8). First, (A.8) seems to ignore the possibility of appearance of new poles, not directly related to the particles A_2 and A_3. It is easy to argue though that such new poles can appear (and indeed do appear) only in the order $O(\eta^2)$, i.e. in $\Phi^{(k)}(\theta)$ with $k \geq 2$ in (A.4). Assume that a new pole appears in $\Phi^{(1)}(\theta)$ at $\theta = \theta_{\text{new pole}}$ within the strip $-\pi \leq \Im m\,\theta \leq 0$ in the complex θ-plane. Obviously, it has to be accompanied by a new zero at $\theta = \theta_{\text{new zero}}$, close to the new pole, $\theta_{\text{new zero}} - \theta_{\text{new pole}} \sim \eta$, so that the pole disappears at $\eta = 0$. The position of the new pole can't be deep inside the above strip, because then the associated zero would lead to a pole within the physical strip $0 < \Im m\,\theta < \pi$, as dictated by the first equation in (A.1).[10] This would imply appearance of a singularity in the upper half-plane of the complex energy, incompatible with the physical requirement of macro causality [25] (the statement that the scattering amplitudes can not have singularities on the principal sheet of the energy surface). Therefore, the new pole can only appear close to the boundary $\Im m\,\theta = 0$ or π, so that the associated new zero would be located in the physical strip $0 < \Im m\,\theta < \pi$. In this case the pole $\theta_{\text{new pole}}$ would signal a conventional resonance state, with the width proportional to the separation between the new pole and the associated new zero. This interpretation immediately rules out possibility of emergence of the new poles in the order η, since then by continuation to the opposite sign of η one could make

---

[10]For more details on possible locations of poles and zeroes of the elastic $2 \to 2$ amplitude see e.g. [9–11].

the width negative, in contradiction with unitarity.[11] To summarize, no additional poles in the finite part of the θ-plane can appear in $\Phi^{(1)}(\theta)$.

Another possible objection concerns asymptotic $\theta \to \infty$ behavior of $S_{11}(\theta)$ in the order $\sim \eta$. Without violation of crossing and unitarity one can add to (A.6) an entire function of θ, subject to the conditions (A.1). Since those conditions suggest $2\pi i$ periodicity of the amplitude, such additional entire function could be either a constant (impossible, as it would violate the condition $S_{11}(0) = -1$), or grow at least as $\sinh\theta$ as $\theta \to \infty$. However, analysis of the form factor perturbation theory suggested that the corrections $\Phi^{(k)}(\theta)$ decay as $\theta^{k-1} e^{-\theta}$ as $\theta \to +\infty$; in particular $\Phi^{(1)}(\theta)$ behaves as $e^{-\theta}$ in this limit, as (A.8) obviously does. Indeed, as $S_{11}(\infty) = +1$, at high energies the particles A_1 behave much like free bosons. In particular, the form factors $\langle A_1(\theta_1)\dots A_1(\theta_N) \mid O_R(0) \mid A_1(\theta'_1)\dots A_1(\theta'_M)\rangle$ of any relevant field operator $O_R(x)$ are bounded by a constant; the above asymptotic behavior of $\Phi^{(n)}(\theta)$ follows.

B Finite-Size corrections to mass gap

Consider a generic 2d massive QFT, and denote A_a the stable particles of the theory, and M_a their masses. We assume that A_1 is the lightest particle in the spectrum. If one puts this theory in the geometry of a cylinder $x \sim x+R$, the energy spectrum acquires the finite size corrections. Thus, the leading large-R correction to the ground state energy is

$$E_0(R) = FR - \sum_a M_a \int \frac{d\theta}{2\pi} e^{-M_a R \cosh\theta} \cosh\theta + \cdots, \tag{B.1}$$

where F is the bulk vacuum energy density. Furthermore, if $E_1(R)$ is the energy of the state of one particle A_1 at rest (see e.g. [27])

$$E_1(R) = FR + M_1 + \sum_{b,c} M_1 \kappa^1_{bc} e^{-\mu^1_{bc} R} - \sum_a M_a \int \frac{d\theta}{2\pi} e^{-M_a R \cosh\theta} S_{1a}\left(\theta + \frac{\pi i}{2}\right) \cosh\theta, \tag{B.2}$$

The sum in the first line here includes particles a, b whose masses satisfy the inequality $M_1^2 \geq |M_a^2 - M_b^2|$, and

$$\mu^a_{bc} = \frac{M_b M_c}{M_a} \sin u^a_{bc}, \qquad \kappa^a_{bc} = -(\Gamma^a_{bc})^2 \, \mu^a_{bc}/M_a, \tag{B.3}$$

Here $i u^c_{ab}$ is the rapidity position of the pole associated with A_c in the amplitude $S_{ab}(\theta)$ of the elastic process $A_a + A_b \to A_a + A_b$,

$$M_c^2 = M_a^2 + M_b^2 + 2 M_a M_b \cos u^c_{ab}, \tag{B.4}$$

and

$$\left(\Gamma^c_{ab}\right)^2 = -i \operatorname*{Res}_{\theta \to i u^c_{ab}} S_{ab}(\theta). \tag{B.5}$$

---

[11]Resonance poles can appear in $S_{11}(\theta)$, and indeed do appear, in the order η^2, see e.g. [26].

In the E_8 theory in section 5 we have $M_2 = 2M_1 \cos \frac{\pi}{5}$ and $M_3 = 2M_1 \cos \frac{\pi}{30}$, and

$$\mu_{22}^1 = \frac{\sqrt{5 + 2\sqrt{5}}}{2} M_1 \approx 1.53884\, M_1\,, \quad \mu_{33}^1 = \frac{1}{2}\sqrt{7 + 8\cos\frac{\pi}{15}} M_1 \approx 1.92517\, M_1\,. \quad \text{(B.6)}$$

This leads to the fitting formula (5.8).

Open Access. This article is distributed under the terms of the Creative Commons Attribution License (CC-BY 4.0), which permits any use, distribution and reproduction in any medium, provided the original author(s) and source are credited.

References

[1] P. Fonseca and A. Zamolodchikov, *Ising field theory in a magnetic field: analytic properties of the free energy*, *J. Stat. Phys.* **110** (2003) 527.

[2] H.-L. Xu and A. Zamolodchikov, 2*D Ising Field Theory in a magnetic field: the Yang-Lee singularity*, *JHEP* **08** (2022) 057 [arXiv:2203.11262] [ɪɴSPIRE].

[3] G. Johnson, F. Rennecke and V.V. Skokov, *Universal location of Yang-Lee edge singularity in classic O(N) universality classes*, *Phys. Rev. D* **107** (2023) 116013 [arXiv:2211.00710] [ɪɴSPIRE].

[4] M. Lencsés, A. Miscioscia, G. Mussardo and G. Takács, *Multicriticality in Yang-Lee edge singularity*, *JHEP* **02** (2023) 046 [arXiv:2211.01123] [ɪɴSPIRE].

[5] I.R. Klebanov, V. Narovlansky, Z. Sun and G. Tarnopolsky, *Ginzburg-Landau description and emergent supersymmetry of the* (3, 8) *minimal model*, *JHEP* **02** (2023) 066 [arXiv:2211.07029] [ɪɴSPIRE].

[6] J. Cardy, *The Yang-Lee Edge Singularity and Related Problems*, arXiv:2305.13288 [ɪɴSPIRE].

[7] C.-N. Yang and T.-D. Lee, *Statistical theory of equations of state and phase transitions. Part 1. Theory of condensation*, *Phys. Rev.* **87** (1952) 404 [ɪɴSPIRE].

[8] T.-D. Lee and C.-N. Yang, *Statistical theory of equations of state and phase transitions. Part 2. Lattice gas and Ising model*, *Phys. Rev.* **87** (1952) 410 [ɪɴSPIRE].

[9] A. Zamolodchikov, *Ising Spectroscopy. Part II. Particles and poles at* $T > T_c$, arXiv:1310.4821 [ɪɴSPIRE].

[10] B. Gabai and X. Yin, *On the S-matrix of Ising field theory in two dimensions*, *JHEP* **10** (2022) 168 [arXiv:1905.00710] [ɪɴSPIRE].

[11] A. Zamolodchikov and I. Ziyatdinov, *Inelastic scattering and elastic amplitude in Ising field theory in a weak magnetic field at* $T > T_c$: *Perturbative analysis*, *Nucl. Phys. B* **849** (2011) 654 [arXiv:1102.0767] [ɪɴSPIRE].

[12] B.M. McCoy and T.T. Wu, *The two-dimensional Ising model*, Courier Corporation (2014).

[13] A. Zamolodchikov, *Integrals of Motion and S Matrix of the (Scaled)* $T = T_c$ *Ising Model with Magnetic Field*, *Int. J. Mod. Phys. A* **4** (1989) 4235 [ɪɴSPIRE].

[14] V.V. Mangazeev, B. Hagan and V.V. Bazhanov, *Corner Transfer Matrix Approach to the Yang-Lee Singularity in the* 2*D Ising Model in a magnetic field*, in preparation (2023).

[15] M.E. Fisher, *Yang-Lee Edge Singularity and ϕ^3 Field Theory*, *Phys. Rev. Lett.* **40** (1978) 1610 [InSPIRE].

[16] J.L. Cardy, *Conformal Invariance and the Yang-Lee Edge Singularity in Two-dimensions*, *Phys. Rev. Lett.* **54** (1985) 1354 [InSPIRE].

[17] J.L. Cardy and G. Mussardo, *S Matrix of the Yang-Lee Edge Singularity in Two-Dimensions*, *Phys. Lett. B* **225** (1989) 275 [InSPIRE].

[18] F. Smirnov and A. Zamolodchikov, *On space of integrable quantum field theories*, *Nucl. Phys. B* **915** (2017) 363 [arXiv:1608.05499] [InSPIRE].

[19] A. Cavaglià, S. Negro, I.M. Szécsényi and R. Tateo, *$T\bar{T}$-deformed 2D Quantum Field Theories*, *JHEP* **10** (2016) 112 [arXiv:1608.05534] [InSPIRE].

[20] S. Dubovsky, V. Gorbenko and M. Mirbabayi, *Asymptotic fragility, near AdS_2 holography and $T\bar{T}$*, *JHEP* **09** (2017) 136 [arXiv:1706.06604] [InSPIRE].

[21] D. Menskoy, F. Smirnov, H. Xu and A. Zamolodchikov, *Ising Field Theory in a Magnetic Field: Inelastic Effects at Pure Imaginary Field*, in preparation (2023).

[22] V.P. Yurov and A. Zamolodchikov, *Truncated conformal space approach to scaling Lee-Yang model*, *Int. J. Mod. Phys. A* **5** (1990) 3221 [InSPIRE].

[23] G. Camilo, T. Fleury, M. Lencsés, S. Negro and A. Zamolodchikov, *On factorizable S-matrices, generalized TTbar, and the Hagedorn transition*, *JHEP* **10** (2021) 062 [arXiv:2106.11999] [InSPIRE].

[24] G. Delfino, G. Mussardo and P. Simonetti, *Nonintegrable quantum field theories as perturbations of certain integrable models*, *Nucl. Phys. B* **473** (1996) 469 [hep-th/9603011] [InSPIRE].

[25] D. Iagolnitzer, *Analyticity properties of the S-matrix: historical survey and recent results in S-matrix theory and axiomatic field theory*, in *New Developments in Mathematical Physics*, Springer (1981), pp. 235–328 [DOI:10.1007/978-3-7091-8642-8_8].

[26] G. Delfino, P. Grinza and G. Mussardo, *Decay of particles above threshold in the Ising field theory with magnetic field*, *Nucl. Phys. B* **737** (2006) 291 [hep-th/0507133] [InSPIRE].

[27] T.R. Klassen and E. Melzer, *On the relation between scattering amplitudes and finite size mass corrections in QFT*, *Nucl. Phys. B* **362** (1991) 329 [InSPIRE].